Synthetic and Systems Biotechnology 9 (2024) 809–819

Contents lists available at ScienceDirect

Synthetic and Systems Biotechnology

journal homepage: www.keaipublishing.com/en/journals/synthetic-and-systems-biotechnology

Original Research Article

Enhanced triacylglycerol metabolism contributes to the efficient biosynthesis of spinosad in *Saccharopolyspora spinosa*

Li Cao, Yangchun Liu, Lin Sun, Zirong Zhu, Danlu Yang, Ziyuan Xia, Duo Jin, Zirui Dai, Jie Rang, Liqiu Xia *

Hunan Provincial Key Laboratory for Microbial Molecular Biology, State Key Laboratory of Development Biology of Freshwater Fish, College of Life Science, Hunan Normal University, Changsha, Hunan, 410081, China

ARTICLE INFO

Keywords:
Saccharopolyspora spinosa
Spinosad
Triacylglycerol
Lipase
Acyl-CoAs

ABSTRACT

Triacylglycerol (TAG) is crucial for antibiotic biosynthesis derived from *Streptomyces*, as it serves as an important carbon source. In this study, the supplementation of exogenous TAG led to a 3.92-fold augmentation in spinosad production. The impact of exogenous TAG on the metabolic network of *Saccharopolyspora spinosa* were deeply analyzed through comparative proteomics. To optimize TAG metabolism and enhance spinosad biosynthesis, the lipase-encoding genes *lip*886 and *lip*385 were overexpressed or co-expressed. The results shown that the yield of spinosad was increased by 0.8-fold and 0.4-fold when *lip*886 and *lip*385 genes were overexpressed, respectively. Synergistic co-expression of these genes resulted in a 2.29-fold increase in the yield of spinosad. Remarkably, the combined overexpression of *lip*886 and *lip*385 in the presence of exogenous TAG elevated spinosad yields by 5.5-fold, led to a drastic increase in spinosad production from 0.036 g/L to 0.234 g/L. This study underscores the modification of intracellular concentrations of free fatty acids (FFAs), short-chain acyl-CoAs, ATP, and NADPH as mechanisms by which exogenous TAG modulates spinosad biosynthesis. Overall, the findings validate the enhancement of TAG catabolism as a beneficial strategy for optimizing spinosad production and provide foundational insights for engineering secondary metabolite biosynthesis pathways in another *Streptomyces*.

1. Introduction

Actinobacteria is one of the main producers of new antibiotics, among which *Streptomyces*, a filamentous Gram-positive actinomycete, remains the largest producer of new and innovative secondary metabolites with bioactive [6]. Polyketides synthesized by *Streptomyces* are typically produced through multi-modular polyketide synthase (PKS) complexes, encoded by extensive biosynthetic gene clusters (BGCs). These complexes utilize short-chain acyl-CoA substrates as both starting and extender units, employing iterative decarboxylative condensations to progressively elaborate the carbon backbone of the resultant polyketide structure [23,27,32,34]. Due to their excellent biological activity, these secondary metabolites are widely used in agriculture and clinical fields [18,27,47,51]. *Streptomyces* undergoes a transition from primary metabolism to secondary metabolism during the fermentation process, and all secondary metabolites are synthesized based on the products of primary metabolism [49]. Understanding how metabolism shifts is beneficial for maximizing the production of target secondary metabolites, such as polyketides [8]. Triacylglycerol (TAG) has been observed to accumulate significantly during the primary metabolic phase in *Streptomyces* [43]. Initially, it was believed that TAG accumulation could be crucial for preserving cellular integrity and serving as a carbon reservoir for the biosynthesis of acetic acid-derived antibiotics under conditions of glucose scarcity in the culture medium [30]. In comparative analyses of the model strains *Streptomyces coelicolor* A3(2) and *Streptomyces lividans*, which differ in their actinorhodin (ACT) production capabilities. It was observed that the strain exhibiting robust ACT synthesis demonstrated fewer TAG accumulation. Conversely, the strain with diminished ACT output exhibited higher levels of TAG [7]. In most *Streptomyces*, there is a statistically significant negative Pearson correlation between total lipid content and antibiotic activity, except for a few strains [5]. Recent a study revealed that intracellular TAG accumulated in primary metabolism is degraded during the stationary phase, And this process could channel carbon flux from both intracellular TAG

Peer review under responsibility of KeAi Communications Co., Ltd.
* Corresponding author.
E-mail address: xialq@hunnu.edu.cn (L. Xia).

https://doi.org/10.1016/j.synbio.2024.06.007
Received 22 April 2024; Received in revised form 16 June 2024; Accepted 22 June 2024
Available online 25 June 2024

and extracellular substrates to polyketide biosynthesis, providing more carbon sources for polyketide biosynthesis. By dynamically regulating the degradation of TAG (ddTAG), it can effectively increase the titers of ACT, jadomycin B, oxytetracycline, and avermectin $B1_a$ in *S. coelicolor*, *Streptomyces venezuelae*, *Streptomyces rimosus* and *Streptomyces avermitilis* [43]. This strategy has broad applicability and provides a simple tool for better understanding the TAG metabolism of cells and improving the titers of polyketides in *Streptomyces*. In the oil-preferring industrial *Streptomyces albus* ZD11, enhancing TAG hydrolysis and fatty acid degradation helps improve oil utilization efficiency, thereby providing abundant carbon precursors for cell growth and salinomycin biosynthesis [20]. The correlation between TAG metabolism and antibiotic biosynthesis is further illustrated. Vegetable oil, primarily composed of triacylglycerol (TAG), serves as an effective carbon source for microbial fermentation processes [3,4]. During metabolism, microorganisms secrete lipase and esterase enzymes, which hydrolyze the vegetable oil into free fatty acids (FFAs) and glycerol. These FFAs are then transported into the cells either through passive diffusion or via protein-facilitated transport mechanisms, Once inside the cell, FFAs are activated by fatty acyl-CoA synthetase (ACS) to form fatty acyl-CoA, which is subsequently funneled into the β-oxidation pathway. Repeated cycles of β-oxidation generate substantial quantities of acetyl-CoA, reducing equivalents, and ATP [20,42]. The accumulation of these reducing equivalents and ATP can inhibit the activities of key enzymes in the tricarboxylic acid (TCA) cycle, including α-ketoglutarate dehydrogenase (KGDH), isocitrate dehydrogenase (IDH), and citrate synthase (CS). This inhibition reduces the flux of acetyl-CoA into the TCA cycle, thereby allowing greater carbon flux towards the biosynthesis of polyketides [43].

Spinosad, a novel eco-friendly insecticide, is synthesized through the aerobic fermentation of the soil-dwelling actinomycete, *Saccharopolyspora spinosa*. It is extensively employed in agriculture for the effective management of a broad spectrum of pest [41]. Spinosad, a macrolide compound, is characterized by a 21-carbon, tetracyclic lactone structure. Attached to the polyketide skeleton at positions 9 and 17 are the deoxysugars tri-O-methylated rhamnose and forosamine, respectively [13]. Typically, spinosad is a composite of two major components: spinosyn A, which constitutes approximately 85 %, and spinosyn D, making up about 15 %. The primary structural distinction between spinosyn D and A is the presence of a single methyl substituent at the 6-position of the polyketide backbone [25]. However, achieving the production targets for spinosad using *S. spinosa* remains a significant challenge due to limited yields. Consequently, efforts to enhance the yield of spinosad are at the forefront of current research endeavors. Current strategies to enhance spinosad yield primarily involve approaches such as heterologous biosynthesis [19,35], metabolic engineering [1], omics analysis [26], and a Combination strategy of heterologous expression, omics analysis, and module optimization [36]. As a secondary metabolite, the biosynthetic pathway of spinosad closely parallels that of other antibiotics derived from *streptomyces*, including avermectin [11], salinomycin [44], and erythromycin [46]. These pathways predominantly utilize short-chain acyl-CoAs as starter and extender units, with biosynthesis occurring predominantly during the mid to late stages of fermentation [21]. Multi-omics analysis has elucidated a close linkage between spinosad biosynthesis and the primary metabolism of *S. spinosa*. The primary metabolism furnishes a copious supply of precursors and energy, which are essential for the efficient biosynthesis of spinosad [26,33].

Spinosad as a typical type I polyketide, it is speculated that enhancing the TAG metabolism can also increase the yield of spinosad though enhancing the precursor supply (Fig. 1A). The correlation between fatty acids and the biosynthesis of spinosad has been established. The supplementation of exogenous fatty acids, specifically a 2:1 ratio of oleic acid to linoleic acid, has been shown to promote spinosad production [45]. This suggests that oleic acid may play a more crucial role in the biosynthesis of spinosad. Vegetable oil is not only an important source of TAG but also a good defoamer, adding soybean oil to the bioreactor can increase the dissolved oxygen [14]. In order to explore

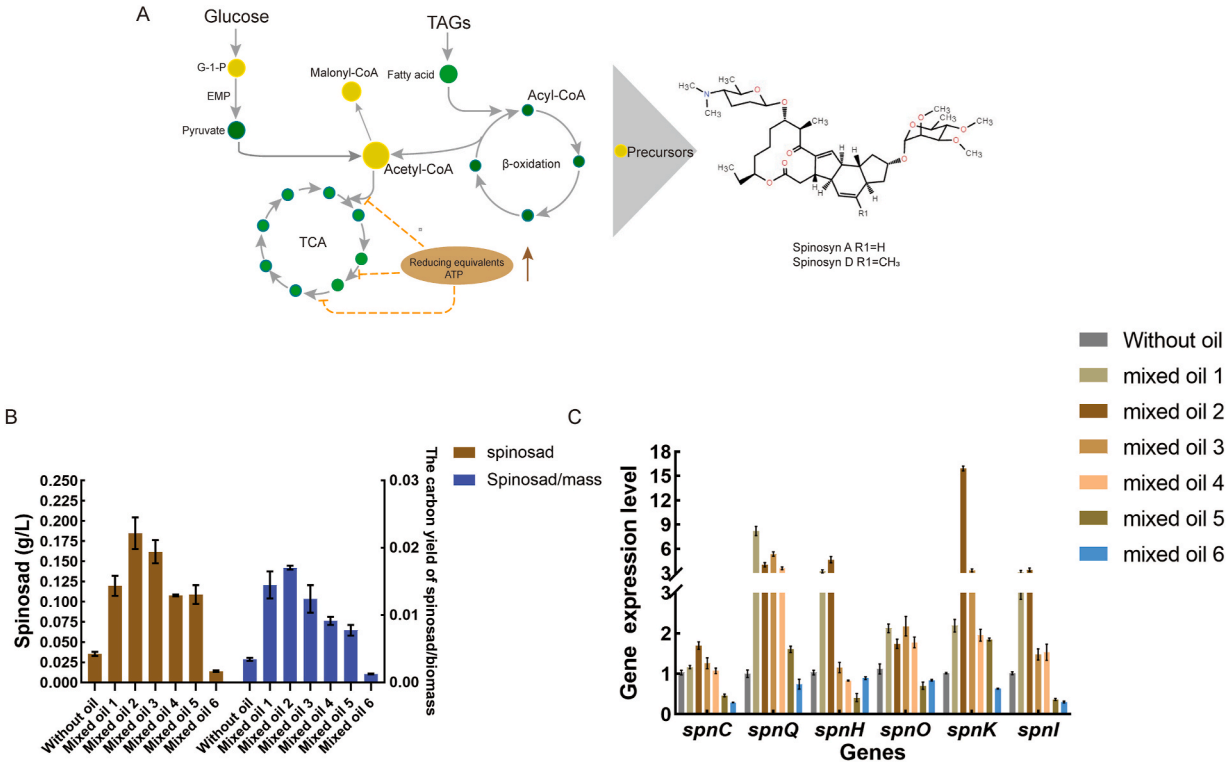

Fig. 1. Schematic diagram of the relationship between TAG metabolism and spinosad biosynthesis and effect of exogenous TAG on spinosad production. (A) Schematic diagram of the relationship between TAG metabolism and spinosad biosynthesis. (B) The yield of spinosad and the carbon yield of spinosad/biomass after adding 30 g/L different mixed oils. (C) The expression levels of spinosad BGC related genes after adding 30 g/L different mixed oils.

the effects of different vegetable oils on the synthesis of spinosad. Rapeseed oil, soybean oil, peanut oil, sesame oil, cottonseed oil, strawberry seed oil and castor oil currently available in the market were selected to mix at a ratio of 1:1 according to the content of oleic acid and linoleic acid, and six different mixed oils were obtained (Tables S3 and S4). Utilizing quantitative proteomics, the influence of mixed oil on the global metabolic network and spinosad biosynthesis in *S. spinosa* CCTCC M206084 has been comprehensively analyzed. To enhance oil metabolism and subsequently increase spinosad production, we employed the PkasO* strong promoter to boost endogenous lipases expression in *S. spinosa*. The impact of these lipases on oil metabolism and spinosad biosynthesis was subsequently investigated.

2. Material and methods

2.1. Strains, plasmids, primers, medium and culture condition

The strains, plasmids, primers, and mixed oils used in this study are listed in Table S1, Table S2, Table S3, and Table S4 of the supporting information. All *Escherichia coli* strains were cultured in LB broth at 37 °C and 250 rpm. The mediums used for the activation and fermentation of *S. spinosa* and its derived strains were complete synthetic medium (CSM) [37] and SFM [37], respectively. The culture conditions were 30 °C and 250 rpm. Strains containing the pOJ260 vector need to add apramycin (50 μg/mL). In addition, R6 medium [38] was used for intergeneric conjugative transfer between *E. coli* S17-1 and *S. spinosa*.

2.2. Growth curve, pH, glucose consumption, and residual oil detection

The 5 mL of bacterial broth is collected every 24 h to measure the growth curve, pH, glucose consumption, and residual oil concentration. The pH value was detected by a pH meter. Similarly, 3,5-dinitrosalicylic acid (DNS) measured the remaining glucose content. The oil concentration was measured by a solvent extraction method [3]. Finally, the bacterial broth was centrifuged to obtain bacterial precipitates for cell dry weight determination.

2.3. Lipase activity assay

The extracellular lipase activity was determined by 4-nitrophenol (*p*-NP) method [40]. 0.1 mL fermentation supernatant was added to 0.2 mL substrate buffer containing 50 mmol/L *p*-nitrophenol palmitate (*p*-NPP), and the reaction was shaken at 37 °C for 15 min. The reaction was terminated by adding 0.7 mL ethanol, and the absorbance at 410 nm was measured. Lipase activity unit (U) was defined as the amount of enzyme required to catalyze the hydrolysis of *p*-NPP to yield 1 μmol *p*-NP per minute.

2.4. Spinosad detected by UHPLC

The fermentation broth on the 12th day was treated with an equal volume of methanol for 8–10 h, then the methanol was removed by a freeze concentrator. Then, an equal volume of ethyl acetate was added for shaking treatment for approximately 5 h. After standing for 30 min and centrifugation, the ethyl acetate layer was removed by vacuum centrifugal concentrator. Finally, the sample was dissolved in 50 μL methanol. The sample dissolved in methanol was detected by ultrahigh-performance liquid chromatograph (UHPLC, Agilent 1290, C18 column: aq12s05-1546, YMC, Japan). The detection wavelength was 250 nm, mobile phase A was 10 % (v/v) methanol, mobile phase B was 90 % (v/v) methanol, the sample loading volume was 20 μL, the elution flow rate was 1 mL/min, and the program ran for 30 min [2]. The titer of spinosad was calculated by the spinosad standard (Purchased from MERCK) (Fig. S8).

2.5. LC−MS/MS detection of protein samples and bioinformatic analysis

Whole protein samples were detected using high pH reversed-phase chromatograph (Thermo Ultimate 3000 UHPLC, ZORBAX Extended-C18) and Q Exactive mass spectrometer (Thermo Scientific, USA; Acclaim PepMap RSLC,75 μmol × 25 cm C18-2 μmol) by a linear gradient at 0.3 mL/min. The detection conditions were as follows: Buffer A was 10 mM ammonium formate, 5 % acetonitrile, pH = 10.0, and buffer B was 10 mM ammonium formate, 90 % acetonitrile, pH = 10.0. The MASCOT engine (embedded in Proteome Discoverer version 1.4 software) was used to identify and quantitatively analyze the raw MS data of each sample.

Differentially expressed proteins (DEPs) were defined as those having several unique peptides ≥1, a fold-change >5 or <0.2, and a P value < 0.05. The DEPs present in the three replicate samples were used for subsequent analysis. The GO database (http://www.geneontology.org/) was used to annotate the DEPs, and the metabolic network related to DEPs was constructed based on the KEGG database (http://www.genome.jp/kegg/).

2.6. Intracellular short-chain acyl-CoAs, ATP, NADPH, and free fatty acid detection

To analyze intracellular levels of short-chain acyl-CoAs, ATP, NADPH, and free fatty acid. The fermentation broth was collected on the fourth and eighth days of fermentation, centrifuged to obtain 0.1 g of bacterial particles, ground into powder with liquid nitrogen, and added 1 mL physiological saline, sonicated for 10 min, centrifuged at 12000 rpm for 10 min, and the supernatant was stored at −80 °C for the detection assays of short-chain acyl-CoAs, ATP, NADPH and free fatty acid. the detection assays referred to the microorganism acetyl-CoA, malonyl-CoA, methylmalonyl-CoA, ATP, and NADPH Elisa assay kit (Jingmei Biotechnology, China) and the method described by Tang et al. [37]. The detection assay of free fatty acid referred to the free fatty acid assay kit (Jingmei Biotechnology, China).

2.7. Construction of recombinant plasmids and strains for lipase overexpression

The process of constructing recombinant vectors and engineered strains were illustrated in Fig. S5. For the recombinant plasmids. Firstly, the P_{kasO*} fragment was amplified by the primer pair PkasO*-F/PkasO*-R with PIB139 as the template. Secondarily, the *lip*385 and *lip*886 genes were amplified by the primer pairs *lip*886-F/*lip*886-R and *lip*385-F/*lip*385-R using the genome of *S. spinosa* as a template. Then, by overlapping extension polymerase chain reaction (PCR) to obtain the PkasO*-*lip*385 and PkasO*-*lip*886 fusion fragments. Finally, the fusion fragments were inserted into the pOJ260 vector by *Xba* I and *Hind* III to obtain the pOJ260-PkasO*-*lip*385 and pOJ260-PkasO*-*lip*886 recombinant vectors (Figs. S6A and B). Similarly, the recombinant vector of the *lip*385 and *lip*886 coexpression was constructed. Firstly, the PkasO*-*lip*385 fragment was amplified by the primer pair PkasO*-*lip*385-F_{co}/*lip*385-R_{co} with pOJ260-PkasO*-*lip*385 as the template. Meantime, the *lip*886 fragment was amplified by the primer pair *lip*886-F_{co}/*lip*886-R_{co}. Secondarily, the PkasO*-*lip*385-*lip*886 (PkasO*-*lip*385-886) was obtained by overlapping extension PCR. Finally, the PkasO*-*lip*385-*lip*886 fragment was inserted into the pOJ260 vector by *Xba* I and *Hind* III to obtain the pOJ260-PkasO*-*lip*385-886 recombinant vector (Figs. S7A, B, C). All recombinant plasmids were again verified by sequencing.

The all-recombinant vectors were integrated into *S. spinosa* by intergeneric conjugative transfer between *S. spinosa* and *E. coli* S17-1. To verify that *lipases* were successfully overexpressed in *S. spinosa.* The PkasO*-*lipase* and PkasO*-*lip*385-886 fusion fragments were amplified by primer pairs PkasO*-F/*lip*385-R, PkasO*-F/*lip*886-R, and PkasO*-*lip*385-F_{co}/*lip*886-R_{co}, respectively. In addition, the expression levels of *lip*385 and *lip*886 genes in related recombinant strains was further

analyzed by qRT-PCR (Figs. S6C, D, E; Figs. S7D and E).

2.8. Total RNA extraction and qRT-PCR analysis

To analyze the transcript level of target genes, the biomass samples from different strains were treated with TotalRNAextractor reagent to obtain total RNA. The concentration and purity of extracted RNA was analyzed using NanoDrop 2000 (Thermo Fisher), and 1ug total RNA was used to synthesize cDNA using a reverse transcription kit (Thermo Fisher), and stored at −80 °C as a template for qRT-PCR. The qRT-PCR analysis was performed using the 7500 Real-Time PCR System instrument (Applied Biosystems, USA), and the SYB® Permix Ex Tag TMGC (Thermo Fisher) was used for qRT-PCR amplification as the fluorescent dye and 16S rRNA as the internal reference to evaluate the expression level of target genes, and three biological replicates were designed.

2.9. Statistical analysis

All data in this study were stated as means ± standard deviation (SD) and analysis by Student' s test, with (*) $p < 0.05$, (**) $p < 0.01$, and (***) $p < 0.001$.

3. Results

3.1. Effects of exogenous triacylglycerol on spinosad biosynthesis, strain growth, and basic carbon source consumption

The effects of different mixed oils on spinosad production, strain growth, pH and glucose consumption during fermentation process were studied. Firstly, the analysis of oil utilization ability showed that *S. spinosa* had good utilization ability for different mixed oils, and most of the mixed oils could be consumed effectively (Fig. S1A). Secondly, the highest yield of spinosad was observed at a concentration of 30 g/L for different mixed oils, and adding mixed oils 2, 3, 1, and 4 at a concentration of 30 g/L resulted in 3.92-fold, 3.47-fold, 2.64-fold, and 2.42-fold increase in the yield of spinosad, respectively, compared to without adding oil (Fig. S1B, Fig. 1B). To analyze the reasons why different exogenous mixed oils affect spinosad biosynthesis. Firstly, the expression levels of spinosad biosynthesis gene cluster (BGC) related genes were analyzed. Since the spinosad BGC consists of 6 transcription units, the *spnC*, *spnQ*, *spnH*, *spnO*, *spnK* and *spnI* genes belong to different transcription unit were selected for analysis [29]. The results demonstrated that the expression levels of *spnC*, *spnQ*, *spnH*, *spnO*, *spnK* and *spnI* genes were upregulated upon the addition of mixture oil 1–4. Notably, the highest upregulation was observed with mixed oils 1 and 2. The difference is that the expression levels of *spnQ* and *spnK* increased while those of other genes decreased following the addition of mixed oil 5. Furthermore, a decrease in expression levels was observed for related genes after adding mixed oil 6 (Fig. 1C). In addition, The biomass, pH, and glucose consumption during the fermentation process of *S. spinosa* supplemented with 30 g/L of different oils were analyzed. Compared with without oil, the addition of mixed oil 1, mixed oil 2, and mixed oil 4 had no significant effect on the biomass of *S. spinosa*. In contrast, the addition of mixed oil 3, mixed oil 5, and mixed oil 6 significantly increased the maximum biomass of *S. spinosa* (Fig. S2A). Meantime, the analysis of spinosad/biomass revealed that the addition of mixed oil 2 also resulted in the highest carbon yield, followed by mixed oil 1 (Fig. 1B). And the addition of various oils did not significantly impact the fermentation process's pH value (Fig. S2B). Glucose, as a basic carbon source, can provide energy and substances for the growth and metabolism of *S. spinosa*. The addition of different oils can accelerate the consumption of basic glucose (Fig. S2C). The above results showed that the effects of vegetable oils on *S. spinosa* are complex.

3.2. Effect of exogenous triacylglycerol on the metabolisms of S. spinosa

Among the various oils tested, the addition of mixed oil 2 resulted in the highest spinosad production, while having no impact on the biomass of *S. spinosa*. To analyze the additional potential influence of exogenous TAG on *S. spinosa*, we used non-labeled data-independent acquisition (DIA) quantitative proteome technology. This allowed us to analyze the difference of protein composition, expression levels, and corresponding biological functions after adding mixed oil 2. Differential expression proteins (DEPs) were identified by screening for Fold Change (FC) greater than 5 times or less than 0.2 times, and a significance P value less than 0.05 using T-test statistics. A total of 896 DEPs were identified from three biological duplicate samples, of these, 684 proteins were upregulated, while 212 proteins were downregulated after mixed oil 2 was added (Figs. S3A and B). The KEGG secondary classification enrichment analysis revealed that 589 DEPs were enriched in global and overview maps. Additionally, 138 DEPs showed enrichment in carbohydrate metabolism, while 124 DEPs exhibited enrichment in amino acid metabolism. Furthermore, the terpenoids and polyketides metabolism pathway was enriched with 73 DEPs, lipid metabolism with 72 DEPs, and both cofactors and vitamins metabolism as well as energy metabolism with 55 DEPs each (Fig. 2A). The KEGG enrichment analysis of the top 25 DEPs revealed that the predominant metabolic pathways encompass secondary metabolite biosynthesis, fatty acid degradation and biosynthesis, amino acid degradation, butanoate metabolism, pyruvate metabolism, glycolysis pathway, and tricarboxylic acid cycle (TCA) (Fig. 2B). Furthermore, the Gene Ontology (GO) enrichment analysis indicated that the DEPs were mainly involved in redox processes and catalytic activity in terms of biological processes and molecular functions, respectively (Fig. 2C). According to the results, the addition of mixed oil 2 exerted a significant impact on the global metabolic network of *S. spinosa* during fermentation. The primary metabolic network diagram was constructed based on the DEPs identified in the comparative proteomics data, including pyruvate metabolism, fatty acid degradation, branched-chain amino acids degradation, and butanoate degradation as the principal sources of acetyl-CoA. Furthermore, a majority of proteins involved in these pathways exhibited upregulation (Fig. 3). Therefore, It is speculated that the addition of mixed oil 2 during the fermentation process primarily affects the availability of acetyl-CoA, thereby influencing spinosad production.

3.3. Effect of exogenous triacylglycerol on the intracellular short-chain acyl-CoAs, ATP, NADPH

The biosynthesis of spinosyn A necessitates one molecule of propionyl-CoA, one molecule of methylmalonyl-CoA and nine molecule of malonyl-CoA as starter and extender units [13]. Therefore, the intracellular availability of short-chain acyl-CoAs is an important factor affecting spinosad biosynthesis. Therefore, the intracellular levels of acetyl-CoA, malonyl-CoA, and methylmalonyl-CoA were quantified on the fourth and eighth days of fermentation to further investigate the impact of exogenous TAG on short-chain acyl-CoAs in *S. spinosa*. The results indicated that there was no statistically significant difference in the levels of acetyl-CoA, malonyl-CoA, and methylmalonyl-CoA on the fourth day of fermentation compared to without oil. However, on the eighth day of fermentation, a decrease in intracellular acetyl-CoA content was observed, while a significant increase in intracellular methylmalonyl-CoA content was noted compared to without oil. (Fig. 4A, B, C). Due to the substantial biosynthesis of spinosad during the intermediate and late stages of fermentation (Fig. S4), it is hypothesized that the cellular level of acetyl-CoA on the 8th day of fermentation was significantly diminished compared to the control group, potentially due to enhanced utilization of acetyl-CoA.

The DEPs enrichment analysis revealed significant enrichments in energy metabolism, fatty acid degradation, pyruvate metabolism, and

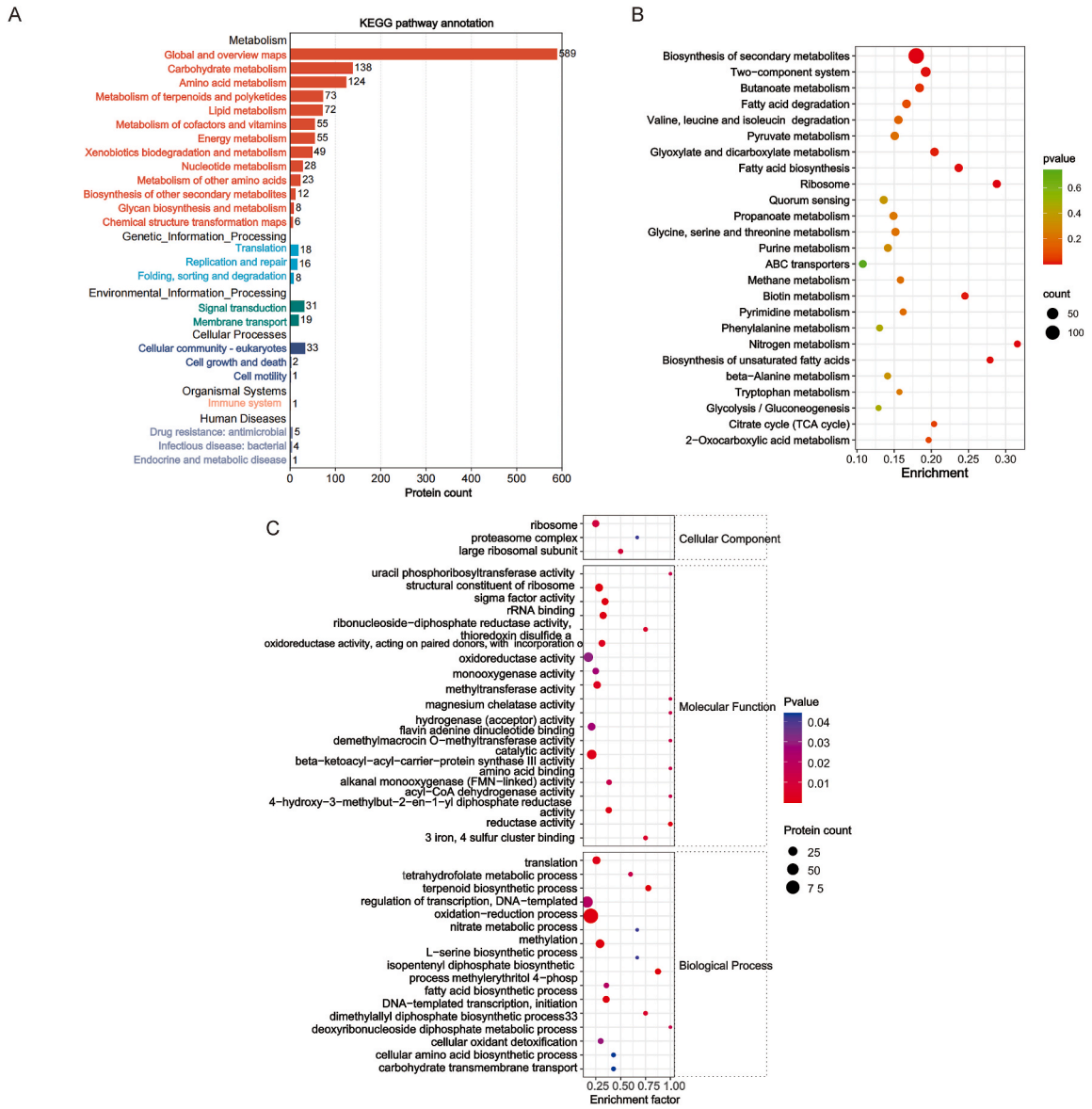

Fig. 2. Comparative proteomics analysis of adding mixed oil 2. (A) KEGG secondary classification enrichment analysis of all DEPs. (B) KEGG enrichment analysis and (C) GO enrichment analysis of the top 25 DEPs. The results from three biological replicates.

branched-chain amino acid degradation pathways, which are known to generate substantial amounts of ATP and reducing equivalents [43]. Therefore, we conducted a quantitative analysis of the intracellular ATP and NADPH levels in biomass samples obtained at 4- and 8-days during fermentation. The results demonstrated that the levels of ATP and NADPH in the fermentation medium containing mixed oil 2 were significantly higher than those observed in the control group on both the fourth and eighth days of fermentation (Fig. 4D and E). The significant increase in spinosad production is speculated to also maybe potentially attributed to the augmentation of intracellular ATP and NADPH levels following the addition of mixed oil 2 into the fermentation medium.

3.4. Engineering strategy of genes encoding lipase increased the yield of spinosad

For vegetable oils can be effectively utilized by microorganisms, they first need to be hydrolyzed to FFAs and glycerol by lipases and esterases secreted by strains, and FFA is then absorbed by cells through passive diffusion and/or protein-facilitated transport, providing a carbon source for microbial growth and metabolism [27]. Quantitative analysis of intracellular free fatty acids (FFAs) content revealed a significant increase in intracellular FFAs upon the addition of mixed oil 2 (Fig. 4F). Additionally, there was an observed elevation in extracellular lipase activity, suggesting that enhanced lipase activity possibly contributed to improved hydrolysis and absorption of exogenous triacylglycerol (Fig. 5A). To gain a deeper understanding of the involvement of lipase in oil utilization and spinosad biosynthesis, we opted to overexpress *lip*886 and *lip*385 genes encoding lipase. Consequently, the corresponding engineered strains were designated as *S. spinosa-lip*886 and *S. spinosa-lip*385. The growth curve, glucose consumption, spinosad production, intracellular short-chain acyl-CoAs, ATP, and NADPH levels were assessed in *S. spinosa-lip*385 and *S. spinosa-lip*886 strains. Biomass accumulation analysis indicated that four days prior to fermentation initiation, the biomass levels of the *S. spinosa-lip*886 and *S. spinosa--lip*385 strains were comparable to those of the wild-type strain. During the mid to late phases of fermentation, the *S. spinosa-lip*385 strain enhanced biomass accumulation and an extended stationary phase compared to the wild-type. Conversely, the *S. spinosa-lip*886 strain transitioned into the decline phase more rapidly than the wild-type (Fig. 5C). Glucose assays conducted during the fermentation process

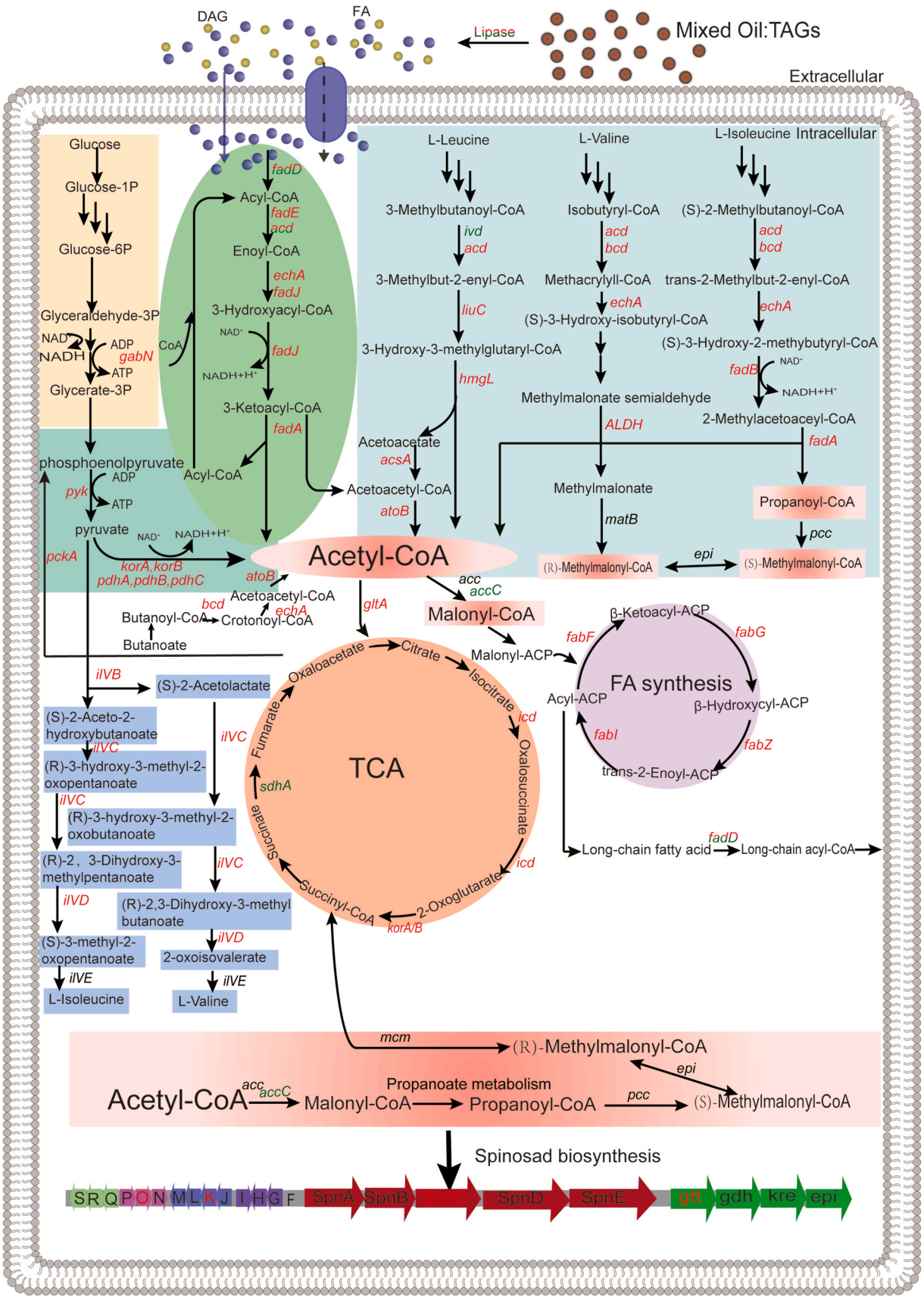

Fig. 3. Metabolic network diagram related to acyl-CoA pools and spinosad biosynthesis Was constructed based on the DEPs identified in the comparative proteomics data. Red represents up-regulated proteins, green represents down-regulated proteins.

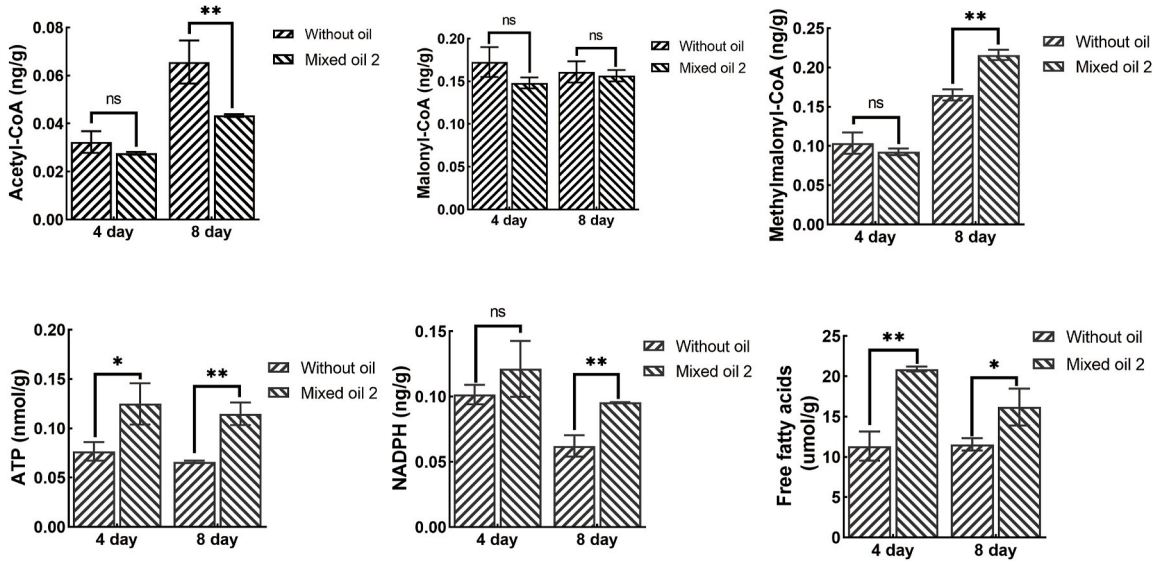

Fig. 4. Effects of mixed oil 2 on the intracellular acyl-CoAs, ATP, NADPH, and FFAs. The levels of intracellular (A) acetyl-CoA, (B) malonyl-CoA, (C) methylmalonyl-CoA, (D) ATP, (E) NADPH, and (F) FFAs. Error bars indicated the standard errors of results from three biological replicates. ,*P < 0.05; **P < 0.01; ***P < 0.001.

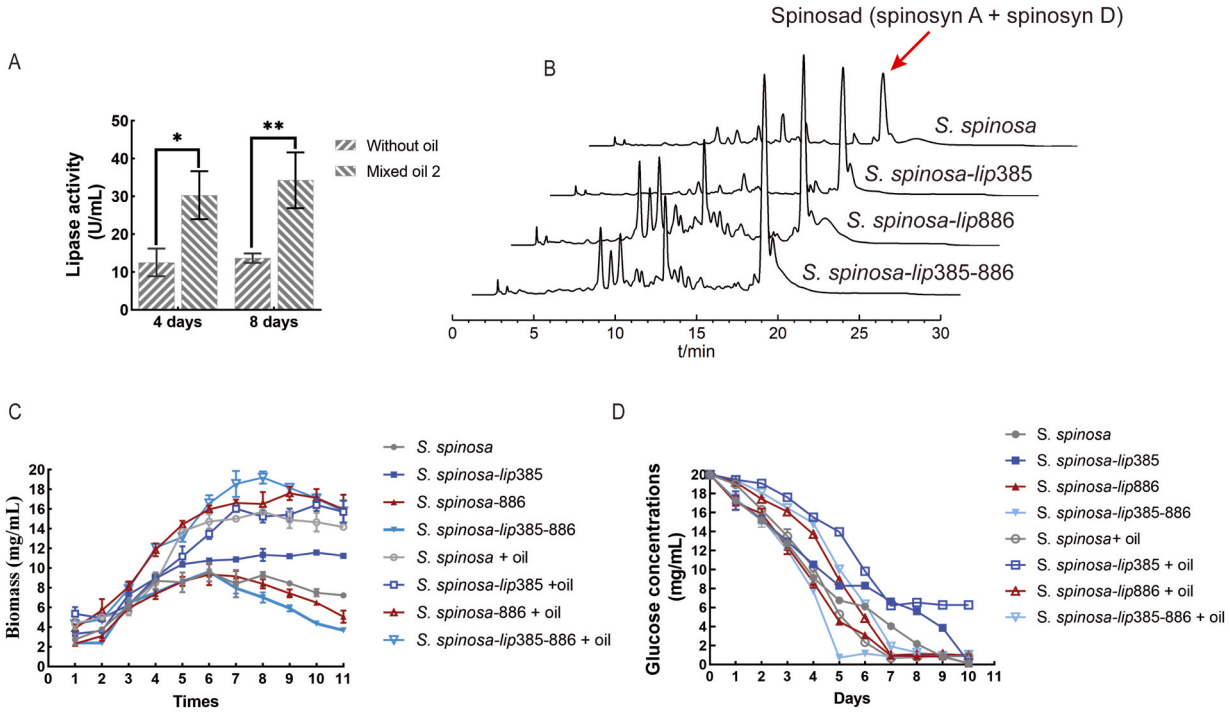

Fig. 5. Effect of lipase on spinosad production, strain growth and glucose consumption. (A) Lipase activity after adding mixed oil. (B) Spinosad production in *S. spinosa-lip*385, *S. spinosa-lip*886, and *S. spinosa-lip*385-886 strains. (C) Biomass of *S. spinosa-lip*385, *S. spinosa-lip*886 and *S. spinosa-lip*385-886 strains in the presence or absence of oil (D) Glucose consumption of *S. spinosa-lip*385, *S. spinosa-lip*886 and *S. spinosa-lip*385-886 strains in the presence or absence of oil. Error bars indicated the standard errors of results from three biological replicates. ,*P < 0.05; **P < 0.01; ***P < 0.001.

indicated that the *S. spinosa-lip*886 strain exhibited a higher rate of glucose consumption compared to the wild-type strain. Conversely, in comparison to the wild-type, the *S. spinosa-lip*385 strain exhibited a slower rate of glucose consumption (Fig. 5D). The analysis of UHPLC revealed 1.8-fold and 1.4-fold increase in spinosad production when *lip*886 and *lip*385 were overexpressed, respectively.(Fig. 5B). To analyze the reasons why lipase affects spinosad biosynthesis. The levels of intracellular short-chain acyl-CoAs, ATP, and NADPH were analyzed. The results showed that the levels of acetyl-CoA and methylmalonyl-CoA in *S. spinosa-lip*886 were higher than those of wild-type strains on the 4th and 8th days of fermentation, while the levels of malonyl-CoA were higher than those of wild-type strains only on the 4th day of fermentation. Compared to the wild type, there were no statistically significant differences in methylmalonyl-CoA content in *S. spinosa-lip*385 on day 4 and day 8 of fermentation. However, the acetyl-CoA content was significantly higher on day 8 of fermentation, while malonyl-CoA content was significantly higher on day 4 of fermentation (Fig. 6A, B, C). The above results showed that the impact of *lip*886 on the accumulation of intracellular short-chain acyl-CoAs was more significant compared to that of *lip*385. The analysis of intracellular

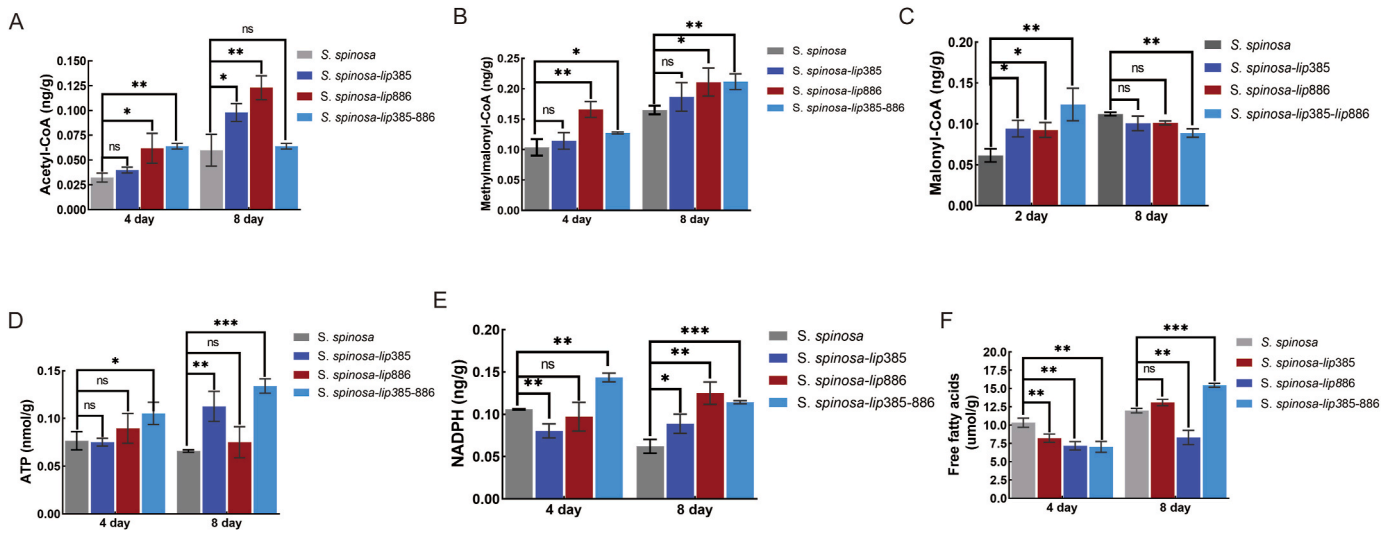

Fig. 6. Effect of lipase on short-chain acyl-CoAs, ATP, NADPH, and intracellular FFAs. The levels of intracellular (A) acetyl-CoA, (B) malonyl-CoA, (C) methylmalonyl-CoA, (D) ATP, (E) NADPH, (F) FFAs in *S. spinosa-lip*385, *S. spinosa-lip*886 and *S. spinosa-lip*385-886 strains. Error bars indicated the standard errors of results from three biological replicates. ,*P < 0.05; **P < 0.01; ***P < 0.001.

ATP and NADPH levels revealed that *S. spinosa-lip*385 exhibited higher levels of ATP and NADPH compared to wild-type strains on the 8th day of fermentation. On the other hand, *S. spinosa-lip*886 only displayed elevated NADPH levels on day 8 of fermentation. (Fig. 6D and E). The above results demonstrated that the impact of *lip*886 on intracellular ATP and NADPH levels was comparatively less significant compared to *lip*385. The analysis of intracellular free fatty acids (FFAs) in *S. spinosa-lip*886 and *S. spinosa-lip*385 strains revealed that the levels of intracellular FFAs were lower in *S. spinosa-lip*886 compared to *S. spinosa* on the 4th and 8th day of fermentation, whereas the levels of intracellular FFAs were significantly higher in *S. spinosa-lip*385 than in *S. spinosa* on the eighth day of fermentation (Fig. 6F). The above findings suggest that the overexpression of *lip*886 promotes intracellular FFAs degradation, whereas the overexpression of *lip*385 results in FFA accumulation. It is hypothesized that *lip*886 primarily enhances spinosad biosynthesis by modulating the accumulation of short-chain acyl-CoAs and the degradation of FFAs, whereas *lip*385 influences spinosad biosynthesis through its impact on intracellular ATP and NADPH levels.

3.5. Combination engineering strategy of lipase further increased the spinosad production

To further increase the yield of spinosad, *lip*886 and *lip*385 were co-expressed to make full use of their different effects on short-chain acyl-CoAs, ATP, and NADPH in *S. spinosa*, and the engineered strain was named *S. spinosa-lip*385-886. The analysis of the growth curve, glucose consumption and spinosad production in *S. spinosa-lip*385-886 revealed a lower biomass compared to the wild-type strain, however, the rate of glucose consumption was faster than that observed in the wild-type strain (Fig. 5C and D). The spinosad production was further enhanced compared to that of the overexpressing strains with a single lipase gene, resulting in a 2.29-fold increase in spinosad production compared to the wild-type strain (Fig. 5B). The analysis of intracellular FAAs showed that the contents in *S. spinosa-lip*385-886 were significantly lower than *S. spinosa* on the 4th day, while significantly higher than *S. spinosa* on the 8th day (Fig. 6F). This indicates that the coexpression of *lip*385 and *lip*886 result in the accumulation of intracellular FAAs. The analysis of intracellular short-chain acyl-CoAs revealed that the levels of acetyl-CoA, malonyl-CoA, and methylmalonyl-CoA in *S. spinosa-lip*385-886 strains were higher than those observed in wild-type strains on the 4th day of fermentation. Furthermore, only the levels of methylmalonyl-CoA surpassed those of wild-type strains on the 8th day of fermentation. Additionally, on day 8 of fermentation, the *S. spinosa-lip*385-886 strains exhibited a significant increase in intracellular ATP and NADPH levels compared to those observed in wild-type strains (Fig. 6A, B, C, D, E). The results indicated that the co-expression of *lip*886 and *lip*385 promoted the synthesis of short-chain acyl-CoAs, ATP, and NADPH, thereby enhancing spinosad production.

3.6. Combining lipase engineering and exogenous triacylglycerol for the improvement of spinosad production

As exogenous TAG, adding mixed oils to the fermentation medium has a broad impact on the global metabolism of *S. spinosa*. To investigate the effect of exogenous TAG on the synthesis of spinosad in engineering strains with *lipase* overexpression. Selecting mixed oil 1, mixed oil 2, mixed oil 3, and mixed oil 4 that are conducive to the spinosad synthesis as medium additives to analyze the effects of exogenous TAG on the yield of spinosad produced by *S. spinosa-lip*385, *S. spinosa-lip*886 and *S. spinosa-lip*385-886 strains. The results showed that mixed oil 1 and mixed oil 2 can further enhance the ability of *S. spinosa-lip*385 strain to produce spinosad. Compared to the wild-type strain (0.036 g/L) without oil, the yield of spinosad was significantly improved by 4.56-fold and 4.1-fold, respectively, reaching 0.201 g/L and 0.184 g/L when 30 g/L mixed oil 2 and mixed oil 1 were added to the fermentation medium. However, there was no significant difference in spinosad production between the *S. spinosa-lip*886 and the wild-type strains after adding mixed oils (Fig. 7A). When mixed oil 1, mixed oil2, mixed oil 3, and mixed oil 4 were added to the fermentation medium, the yield of spinosad produced the *S. spinosa-lip*385-886 was significantly increased when adding mixed oil 1 to the fermentation medium, which increased by 5.5-fold that of the wild-type strain (0.036 g/L) in the medium without oil, reaching 0.234 g/L (Fig. 7B). Additionally, we conducted further analysis on the impact of incorporating mixed oil on glucose consumption and biomass in *S. spinosa-lip*385, *S. spinosa-lip*886, and *S. spinosa-lip*385-886 strains. The findings revealed that compared to the absence of oil, the addition of mixed oil significantly enhanced biomass and extended the stationary phase duration. Although the rate of glucose consumption slowed down after the addition of oil, except for the *S. spinosa-lip*385 strain, glucose was essentially depleted (Fig. 5C and D). These results indicate that the combination engineering strategy of different lipases can enhance biomass accumulation and further promote spinosad biosynthesis in the presence of exogenous triacylglycerol.

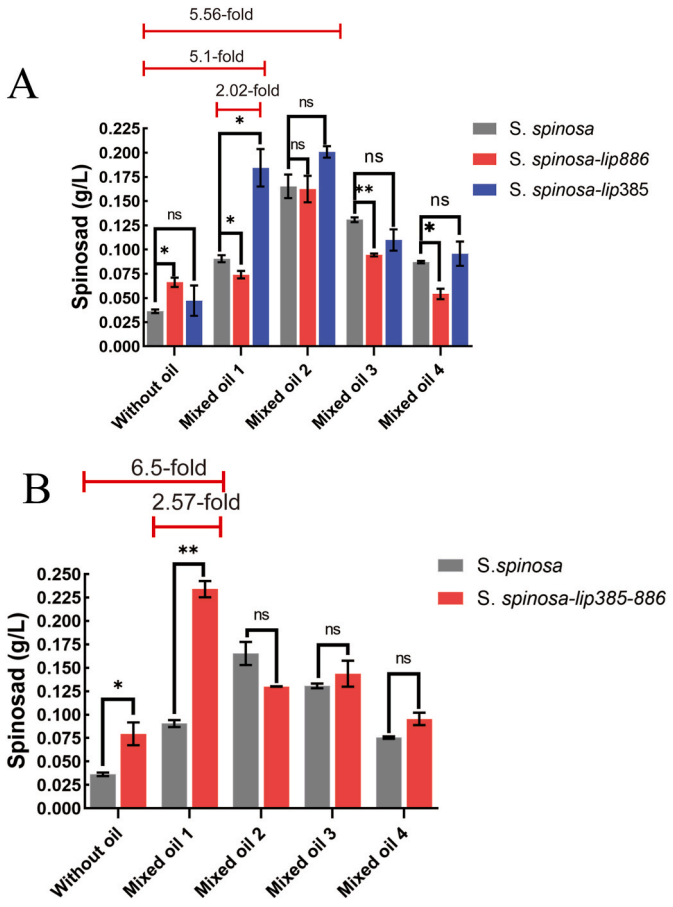

Fig. 7. The yield of spinosad produced by *S. spinosa-lip*385, *S. spinosa-lip*886 and *S. spinosa-lip*385-886 strains adding 30 g/L different mixed oils. (A) Spinosad produced by *S. spinosa-lip*385 and *S. spinosa-lip*886 strains, and (B) Spinosad produced by *S. spinosa-lip*385-886 strain. Error bars indicated the standard errors of results from three biological replicates.

4. Discussion

In this study, the composition of the oil mixture was strategically chosen to emphasize vegetable oils rich in oleic acid due to its favorable impact on metabolic processes. The observed effects of different mixed oils on spinosad production paralleled the influences of oleic acid on Fungichromin synthesis. Notably, Fungichromin, a polyene macrolide antibiotic, exhibits decreased production in the presence of linoleic acid. Conversely, supplementation with oleic acid has been demonstrated to enhance Fungichromin production by 3-fold [48]. The use of diverse oil mixtures was found to enhance glucose consumption, it was speculated that there are two main reasons: both glucose and oils in fermentation media serve as carbon sources, and the cells use both substrates simultaneously, evidently by exclusive mechanisms, with glucose providing all intermediates for the derivation of acetic acid and oils providing straight-chain fatty acyl groups [31]. In addition, in the medium containing oils, the vegetative form of the strain will be prolonged [10]. In summary, the addition of oil possibly increases the demand for glucose in cell growth and metabolism, thus increasing the consumption of glucose. However, they had varying effects on biomass accumulation. Specifically, the addition of mixed oils 3 and 5 was associated with increased biomass, suggesting their potential to boost spinosad yield through enhanced biomass production. In contrast, mixed oils 1, 2, and 4 did not influence biomass levels, implying that they may affect spinosad biosynthesis via alternative pathways. Subsequent quantitative proteomic analysis revealed that vegetable oil significantly impacts the global metabolism of *S. spinosa*. Furthermore, it was demonstrated to augment primary metabolic pathways derived from acetyl-CoA. Essential metabolic processes such as β-oxidation, pyruvate metabolism, amino acid metabolism, and the tricarboxylic acid (TCA) cycle are intricately linked to the production of secondary metabolites in bacteria. These pathways provide a rich supply of precursors and reducing equivalents, crucial for the biosynthesis of polyketides [9,11,26,39]. Acetyl-CoA, originating from primary metabolism, is converted into malonyl-CoA and methylmalonyl-CoA via the acetyl-CoA carboxylase (ACC) and propionyl-CoA carboxylase (PCC) pathways, facilitating its role as a precursor in spinosad biosynthesis [24,28]. However, proteomic analysis did not indicate significant alterations in the expression levels of ACC and PCC-related proteins. Instead, it revealed an enhancement in the catabolism of L-valine and L-isoleucine (Table S5, Fig. 3), suggesting that the increased levels of methylmalonyl-CoA are primarily derived from the breakdown of these amino acids. Consequently, the utilization of vegetable oil is hypothesized to boost the biosynthesis of both acetyl-CoA and methylmalonyl-CoA, thus enhancing the availability of essential precursors and promoting the production of spinosad.

Cofactors play a crucial role in natural product biosynthesis, where the formation of the polyketide skeleton requires a large amount of reducing equivalents [12]. The fluxes directing to NADPH and acetyl-CoA can provide key switches for overall and secondary metabolism [50]. The production of 1 g biomass was calculated to require 39.9 mmol of ATP and 7.5 mmol of NADPH when acetyl-CoA flows into the TCA cycle via citrate synthetase (CS). However, the accumulation of a substantial amount of ATP and reducing equivalents can exert inhibitory effects on the activity of citrate synthase (CS), α-ketoglutarate dehydrogenase (KGDH), and isocitrate dehydrogenase (IDH) in the tricarboxylic acid (TCA) cycle, thereby attenuating metabolic flux towards the TCA cycle and consequently diverting more carbon flux towards polyketide biosynthesis [43]. A study has shown that high levels of NADPH are required in the biosynthesis of penicillin, so the PPP pathway, as one of the major sources of NADPH, increases its flux. When the demand for NADPH decreases, the flux through PPP also decreases [16]. In *Streptomyces lividans* TK24, increasing the concentration of NADPH specifically triggers undecylprodigiosin biosynthesis that required many precursors and NADPH-dependent reduction reaction [15]. Therefore, cells can achieve balance of excessive equivalents through between primary metabolism and secondary generation transition. Erythromycin biosynthesis is positively correlated with intracellular ATP/ADP ratio, optimization of metabolic flow distribution by cofactor engineering is beneficial to increase erythromycin production [22]. It is speculated that the addition of vegetable oil significantly enhances intracellular ATP and NADPH levels, potentially contributing to the observed increase in spinosad production.

In this study, we observed a significant enhancement in extracellular lipase activity upon the addition of vegetable oil. This finding is consistent with previous studies demonstrating that corn oil can induce lipase production in *Streptomyces clavuligerus* CKD 1119 mutant strains, and further supports the positive correlation between lipase activity and tacrolimus (FK-506) production [17]. Lipase, serving as the initial catalyst in oil metabolism, plays an integral role in facilitating the degradation and efficient utilization of oil substrates. Thus, lipase is identified as a key enzyme for enhancing oil metabolism. Through genetic manipulation of lipases, it was observed that various lipases differentially impact spinosad production, as well as the intracellular levels of short-chain acyl-CoAs, ATP, and NADPH. It is believed that the lipases present in *S. spinosa* resemble those described by Han Li et al., where multiple lipases operate synergistically and complementarily to achieve efficient and stable hydrolysis of oil in the medium [27]. In this investigation, the incorporation of mixed oil 1 and mixed oil 2 in the fermentation medium could further enhance the spinosad production in the *S. spinosa-lip*385 strain. Conversely, the spinosad yield in the *S. spinosa-lip886* strain showed no improvement over that of the wild-type strain under similar conditions. To optimize the differential

impacts on oil utilization, as well as on levels of short-chain acyl-CoAs, ATP, and NADPH, the co-expression of *lip*385 and *lip*886 was implemented to boost spinosad production. Compared to strains overexpressing a single lipase, the co-expression strains of *lip*385 and *lip*886 demonstrated enhanced spinosad production, irrespective of the presence of exogenous triacylglycerol (TAG). Consequently, the combinatorial engineering of different lipases represents a potent strategy for augmenting oil metabolism and spinosad synthesis. This approach also offers a promising avenue for the engineering design aimed at improving oil metabolism and the synthesis of other polyketides.

5. Conclusions

In this study, a variety of mixed oils were utilized as additives in the medium to optimize the fermentation process of *S. spinosa*, achieving a significant 3.92-fold increase in spinosad production. The inclusion of these oils markedly influenced the overall metabolism of *S. spinosa*, particularly augmenting primary metabolic pathways involved in acetyl-CoA synthesis. To further enhance spinosad yield, genetic engineering techniques were employed to upregulate the expression of two specific lipase genes. As a result, the introduction of exogenous oil led to a 5.5-fold increase further in spinosad production, demonstrating the efficacy of this integrated biotechnological approach.

CRediT authorship contribution statement

Liqiu Xia conceived of the project. Liqiu Xia and Jie Rang generated ideas and designed research. Li Cao, Yangchun Liu, Zirong Zhu, and Ziyuan Xia performed the HPLC and proteome analysis. Li Cao, Danlu Yang, Zirong Zhu, and Yangchun Liu performed the mutant strain construction. Li Cao, Lin Sun, Duo Jin, and Zirui Dai performed the mutant physiological and short-chain acyl-CoAs, ATP, and NADPH assays. Li Cao, Jie Rang, and Liqiu Xia wrote the manuscript. All authors discussed the results and approved the final manuscript.

Declaration of competing interest

The authors declare that they have no known competing financial interests or personal relationships that could have appeared to influence the work reported in this paper.

Acknowledgements

This work was supported by funding from the National Natural Science Foundation of China (31770106, 32200062) and the Natural Science Foundation of Hunan Province (2024JJ5258).

Appendix A. Supplementary data

Supplementary data to this article can be found online at https://doi.org/10.1016/j.synbio.2024.06.007.

References

[1] Bridget AF, Nguyen CT, Magar RT, Sohng JK. Increasing production of spinosad in *Saccharopolyspora spinosa* by metabolic engineering. Biotechnol Appl Biochem 2022;70(3):1035–43. https://doi:10.1002/bab.2418.

[2] Cao L, Zhu Z, Qin H, Xia Z, Xie J, Li X, Rang J, Hu S, Sun Y, Xia L. Effects of a Pirin-like protein on strain growth and spinosad biosynthesis in *Saccharopolyspora spinosa*. Appl Microbiol Biotechnol 2023;107(17):5439–51. https://doi:10.1007/s00253-023-12636-8.

[3] Choi D-B, Cho K-A. Effect of carbon source consumption rate on lincomycin production from *Streptomyces lincolnensis*. J Microbiol Biotechnol 2004;14(3):532–9.

[4] Choi D, Park S-S, Ahn B-K, Lim D-H, Lee Y-W, Moon J-H, Shin D-Y. Studies on production of gentamicin from Micromonosporas purpurea using crude vegetable oils. Process Biochem 2008;43(8):835–41. https://doi:10.1016/j.procbio.2008.04.010.

[5] David M, Lejeune C, Abreu S, Thibessard A, Leblond P, Chaminade P, Virolle M-J. Negative correlation between lipid content and antibiotic activity in *Streptomyces*: general Rule and Exceptions. Antibiotics 2020;9(6). https://doi:10.3390/antibiotics9060280.

[6] Donald L, Pipite A, Subramani R, Owen J, Keyzers RA, Taufa T. *Streptomyces*: still the biggest producer of new natural secondary metabolites, a current perspective. Microbiol Res 2022;13(3):418–65. https://doi:10.3390/microbiolres13030031.

[7] Esnault C, Dulermo T, Smirnov A, Askora A, David M, Deniset-Besseau A, Holland I-B, Virolle M-J. Strong antibiotic production is correlated with highly active oxidative metabolism in *Streptomyces coelicolor* M145. Sci Rep 2017;7(1). https://doi:10.1038/s41598-017-00259-9.

[8] Gamboa-Suasnavart RA, Valdez-Cruz NA, Gaytan-Ortega G, Reynoso-Cereceda GI, Cabrera-Santos D, López-Griego L, Klöckner W, Büchs J, Trujillo-Roldán MA. The metabolic switch can be activated in a recombinant strain of *Streptomyces lividans* by a low oxygen transfer rate in shake flasks. Microb Cell Factories 2018;17(1). https://doi:10.1186/s12934-018-1035-3.

[9] Gläser L, Kuhl M, Stegmüller J, Rückert C, Myronovskyi M, Kalinowski J, Luzhetskyy A, Wittmann C. Superior production of heavy pamamycin derivatives using a bkdR deletion mutant of *Streptomyces albus* J1074/R2. Microb Cell Factories 2021;20(1). https://doi:10.1186/s12934-021-01602-6.

[10] Hamedi J, Malekzadeh F, Saghafi-nia AE. Enhancing of erythromycin production by *Saccharopolyspora erythraea* with common and uncommon oils. J Ind Microbiol Biotechnol 2004;31(10):447–56. https://doi:10.1007/s10295-004-0166-1.

[11] Hao Y, You Y, Chen Z, Li J, Liu G, Wen Y. Avermectin B1a production in *Streptomyces avermitilis* is enhanced by engineering aveC and precursor supply genes. Appl Microbiol Biotechnol 2022;106(5–6):2191–205. https://doi:10.1007/s00253-022-11854-w.

[12] Huang K, Zhang B, Shen Z-Y, Cai X, Liu Z-Q, Zheng Y-G. Enhanced amphotericin B production by genetically engineered *Streptomyces nodosus*. Microbiol Res 2021;242. https://doi.org/10.1016/j.micres.2020.126623.

[13] Jha AK, Pokhrel AR, Chaudhary AK, Park S-W, Cho WJ, Sohng JK. Metabolic engineering of rational screened *Saccharopolyspora spinosa* for the enhancement of spinosyns A and D production. Mol Cell 2014;37(10):727–33. https://doi:10.14348/molcells.2014.0168.

[14] Jia S, Chen G, Kahar P, Chol DB, Okabez AM. Effect of soybean oil on oxygen transfer in the production of tetracycline with an airlift bioreactor. Ournal Biosci. Bioeng. 1999;87(6):825–7.

[15] Jin X-M, Chang Y-K, Lee JH. Hong S-K Effects of increased NADPH concentration by metabolic engineering of the pentose phosphate pathway on antibiotic production and sporulation in *Streptomyces lividans* TK24. J Microbiol Biotechnol 2017;27(10):1867–76. https://doi:10.4014/jmb.1707.07046.

[16] Jørgensen H, Nielsen J, Villadsen J, Møllgaard H. Metabolic flux distributions in Penicillium chrysogenum during fed-batch cultivations. Biotechnol Bioeng 2004;46(2):117–31. https://doi:10.1002/bit.260460205.

[17] Kim HS, Park YI. Lipase activity and tacrolimus production in *Streptomyces clavuligerus* CKD 1119 mutant strains. J Microbiol Biotechnol 2007;17(10):1638–44.

[18] Kim M-S, Cho W-J, Song MC, Park S-W, Kim K, Kim E, Lee N, Nam S-J, Oh K-H, Yoon YJ. Engineered biosynthesis of milbemycins in the avermectin high-producing strain *Streptomyces avermitilis*. Microb Cell Factories 2017;16(1). https://doi:10.1186/s12934-017-0626-8.

[19] Li H, Pan Y, Liu G. Multiplying the heterologous production of spinosad through tandem amplification of its biosynthetic gene cluster in *Streptomyces coelicolor*. Microb Biotechnol 2021;15(5):1550–60. https://doi:10.1111/1751-7915.13965.

[20] Li H, Wei J, Dong J, Li Y, Li Y, Chen Y, Guan W, Julia Pettinari M. Enhanced triacylglycerol metabolism contributes to efficient oil utilization and high-level production of salinomycin in *Streptomyces albus* ZD11. Appl Environ Microbiol 2020;86(16). https://doi:10.1128/aem.00763-20.

[21] Li S, Wang J, Xiang W, Yang K, Li Z, Wang W. An autoregulated fine-tuning strategy for titer improvement of secondary metabolites using native promoters in *Streptomyces*. ACS Synth Biol 2017;7(2):522–30. https://doi:10.1021/acssynbio.7b00318.

[22] Li X, Chen J, Andersen JM, Chu J, Jensen PR. Cofactor engineering redirects secondary metabolism and enhances erythromycin production in *Saccharopolyspora erythraea*. ACS Synth Biol 2020;9(3):655–70. https://doi:10.1021/acssynbio.9b00528.

[23] Liang L, Haltli B, Marchbank DH, Fischer M, Kirby CW, Correa H, Clark TN, Gray CA, Kerr RG. Discovery of an isothiazolinone-containing antitubercular natural product levesquamide. J Org Chem 2020;85(10):6450–62. https://doi:10.1021/acs.joc.0c00339.

[24] Liu Y, Wang H, Li S, Zhang Y, Cheng X, Xiang W, Wang X. Engineering of primary metabolic pathways for titer improvement of milbemycins in *Streptomyces bingchenggensis*. Appl Microbiol Biotechnol 2021;105(5):1875–87. https://doi:10.1007/s00253-021-11164-7.

[25] Liu Z, Xiao J, Tang J, Liu Y, Shuai L, Cao L, Xia Z, Ding X, Rang J, Xia L. Effects of *acuC* on the growth development and spinosad biosynthesis of *Saccharopolyspora spinosa*. Microb Cell Factories 2021;20(1). https://doi:10.1186/s12934-021-01630-2.

[26] Liu Z, Zhu Z, Tang J, He H, Wan Q, Luo Y, Huang W, Yu Z, Hu Y, Ding X, Xia L. RNA-Seq-based transcriptomic analysis of *Saccharopolyspora spinosa* revealed the critical function of PEP Phosphonomutase in the replenishment pathway. J Agric Food Chem 2020;68(49):14660–9. https://doi:10.1021/acs.jafc.0c04443.

[27] Lu C, Zhang X, Jiang M, Bai L. Enhanced salinomycin production by adjusting the supply of polyketide extender units in Streptomyces albus. Metab Eng 2016;35:129–37. https://doi:10.1016/j.ymben.2016.02.012.

[28] Milke L, Marienhagen J. Engineering intracellular malonyl-CoA availability in microbial hosts and its impact on polyketide and fatty acid synthesis. Appl Microbiol Biotechnol 2020;104(14):6057–65. https://doi:10.1007/s00253-020-10643-7.
[29] Mu X, Lei R, Yan S, Deng Z, Liu R, Liu T. The LysR family transcriptional regulator ORF-L16 regulates spinosad biosynthesis in *Saccharopolyspora spinosa*. Synth. Syst. Biotechnol. 2024;9(4):609–17. https://doi:10.1016/j.synbio.2024.05.001.
[30] Olukoshi ER, Packter NM. Importance of stored triacylglycerols in *Streptomyces* : possible carbon source fo antibiotics. Microbiology 1994;140:931–43.
[31] Peacock L, Ward J, Ratledge C, Dickinson M, Ison A. How *Streptomyces lividans* uses oils and sugars as mixed substrates. Enzym Microb Technol 2003;23:157–66.
[32] Peng H, Ishida K, Sugimoto Y, Jenke-Kodama H, Hertweck C. Emulating evolutionary processes to morph aureothin-type modular polyketide synthases and associated oxygenases. Nat Commun 2019;10(1). https://doi:10.1038/s41467-019-11896-1.
[33] Qi Yang, Ding Xuezhi, Liu Xuemei, Liu Shuang, Sun Yunjun, Yu Ziquan, Hu Shengbiao, Jie Rang, He Hao, Lian He, Xia L. Differential proteomic profiling reveals regulatory proteins and novel links between primary metabolism and spinosad production in *Saccharopolyspora spinosa*. Microb Cell Factories 2014;13(27).
[34] Ray L, Valentic TR, Miyazawa T, Withall DM, Song L, Milligan JC, Osada H, Takahashi S, Tsai S-C, Challis GL. A crotonyl-CoA reductase-carboxylase independent pathway for assembly of unusual alkylmalonyl-CoA polyketide synthase extender units. Nat Commun 2016;7(1). https://doi:10.1038/ncomms13609.
[35] Song C, Luan J, Cui Q, Duan Q, Li Z, Gao Y, Li R, Li A, Shen Y, Li Y, Stewart AF, Zhang Y, Fu J, Wang H. Enhanced heterologous spinosad production from a 79-kb synthetic multioperon assembly. ACS Synth Biol 2018;8(1):137–47. https://doi:10.1021/acssynbio.8b00402.
[36] Tan G-Y, Deng K, Liu X, Tao H, Chang Y, Chen J, Chen K, Sheng Z, Deng Z, Liu T. Heterologous biosynthesis of spinosad: an omics-guided large polyketide synthase gene cluster reconstitution in *Streptomyces*. ACS Synth Biol 2017;6(6):995–1005. https://doi:10.1021/acssynbio.6b00330.
[37] Tang J, He H, Li Y, Liu Z, Xia Z, Cao L, Zhu Z, Shuai L, Liu Y, Wan Q, Luo Y, Zhang Y, Rang J, Xia L. Comparative proteomics reveals the effect of the transcriptional regulator Sp13016 on butenyl-spinosyn biosynthesis in *Saccharopolyspora pogona*. J Agric Food Chem 2021;69(42):12554–65. https://doi:10.1021/acs.jafc.1c03654.
[38] Tang J, Zhu Z, He H, Liu Z, Xia Z, Chen J, Hu J, Cao L, Rang J, Shuai L, Liu Y, Sun Y, Ding X, Hu S, Xia L. Bacterioferritin: a key iron storage modulator that affects strain growth and butenyl-spinosyn biosynthesis in *Saccharopolyspora pogona*. Microb Cell Factories 2021;20(1). https://doi:10.1186/s12934-021-01651-x.
[39] Tian J, Yang G, Gu Y, Sun X, Lu Y, Jiang W. Developing an endogenous quorum-sensing based CRISPRi circuit for autonomous and tunable dynamic regulation of multiple targets in *Streptomyces*. Nucleic Acids Res 2020;48(14):8188–202. https://doi:10.1093/nar/gkaa602.
[40] Tian M, Fu J, Wang Z, Miao C, Lv P, He D, Li Z, Liu T, Li M, Luo W. Enhanced activity and stability of Rhizomucor miehei lipase by mutating N-linked glycosylation site and its application in biodiesel production. Fuel 2021:304. https://doi:10.1016/j.fuel.2021.121514.
[41] Waldron C, Matsushima P, Rosteck Jr PR, Broughton MC, Turner J, Madduri K, Crawford KP, Merlo DJ, Rh B. Cloning and analysis of the spinosad biosynthetic gene cluster of *Saccharopolyspora spinosa*. Chem Biol 2001;8(5):487–99. https://doi:10.1016/s1074-5521(01)00029-1. PMID: 11358695.
[42] Wang S, Deng H. The X-factor: enhanced β-oxidation on intracellular triacylglycerols enabling overproduction of polyketide drug-like molecules in microorganisms. Synth. Syst. Biotechnol. 2020;5(1):19–20. https://doi:10.1016/j.synbio.2020.01.005.
[43] Wang W, Li S, Li Z, Zhang J, Fan K, Tan G, Ai G, Lam SM, Shui G, Yang Z, Lu H, Jin P, Li Y, Chen X, Xia X, Liu X, Dannelly HK, Yang C, Yang Y, Zhang S, Alterovitz G, Xiang W, Zhang L. Harnessing the intracellular triacylglycerols for titer improvement of polyketides in *Streptomyces*. Nat Biotechnol 2019;38(1):76–83. https://doi:10.1038/s41587-019-0335-4.
[44] Wei J, Chen B, Dong J, Wang X, Li Y, Liu Y, Guan W. Salinomycin biosynthesis reversely regulates the β-oxidation pathway in *Streptomyces albus* by carrying a 3-hydroxyacyl-CoA dehydrogenase gene in its biosynthetic gene cluster. Microb Biotechnol 2022;15(12):2890–904. https://doi:10.1111/1751-7915.14145.
[45] Xue C, Zhang X, Yu Z, Zhao F, Wang M, Lu W. Up-regulated spinosad pathway coupling with the increased concentration of acetyl-CoA and malonyl-CoA contributed to the increase of spinosad in the presence of exogenous fatty acid. Biochem Eng J 2013;81:47–53. https://doi:10.1016/j.bej.2013.10.004.
[46] You D, Wang M-M, Yin B-C, Ye B-C. Precursor supply for erythromycin biosynthesis: engineering of propionate assimilation pathway based on propionylation modification. ACS Synth Biol 2019;8(2):371–80. https://doi:10.1021/acssynbio.8b00396.
[47] Yu Z, Lv H, Wu Y, Wei T, Yang S, Ju D, Chen S. Enhancement of FK520 production in *Streptomyces hygroscopicus* by combining traditional mutagenesis with metabolic engineering. Appl Microbiol Biotechnol 2019;103(23–24):9593–606. https://doi:10.1007/s00253-019-10192-8.
[48] Zang C-Z, Chang Y-N, Chen H-B, Wu J-Y, Chen C-I, Huang J-W, Shih H-D, Liu Y-C. Deciphering the roles of fatty acids and oils in fungichromin enhancement from *Streptomyces padanus*. J Taiwan Inst Chem Eng 2011;42(3):413–8. https://doi:10.1016/j.jtice.2010.09.010.
[49] Zhao M, Wang M, Wang S, Xiong L, Gao B, Liu M, Tao X, Wang F-Q, Wei D. A self-sustained system spanning the primary and secondary metabolism stages to boost the productivity of *Streptomyces*. ACS Synth Biol 2021;11(1):353–65. https://doi:10.1021/acssynbio.1c00473.
[50] Zhu X-M, Zhang X-X, Cheng R-T, Yu H-L, Yuan R-S, Bu X-L, Xu J, Ao P, Chen Y-C, Xu M-J. Dynamical modelling of secondary metabolism and metabolic switches in *Streptomyces xiamenensis* 318. R Soc Open Sci 2019;6(4). https://doi.org/10.1098/rsos.190418.
[51] Zou Z, Hu X, Luo T, Ming Z, Chen X, Xia L, Luo W, Li J, Xu N, Chen L, Cao D, Wen M, Kong F, Peng K, Xie Y, Li X, Ma D, Yang C, Chen C, Yi W, Liu O, Liu S, Luo J, Luo Z. Naturally-occurring spinosyn A and its derivatives function as argininosuccinate synthase activator and tumor inhibitor. Nat Commun 2021;12(1). https://doi:10.1038/s41467-021-22235-8.